Zeaxanthin induces Nrf2-mediated phase II enzymes in protection of cell death

X Zou[1,2,5], J Gao[1,3,5], Y Zheng[4], X Wang[1,3], C Chen[1,3], K Cao[1,3], J Xu[1,3], Y Li[1,3], W Lu[1,2], J Liu[1,3] and Z Feng*,[1,3]

Zeaxanthin (Zea) is a major carotenoid pigment contained in human retina, and its daily supplementation associated with lower risk of age-related macular degeneration. Despite known property of Zea as an antioxidant, its underlying molecular mechanisms of action remain poorly understood. In this study, we aim to study the regulation mechanism of Zea on phase II detoxification enzymes. In normal human retinal pigment epithelium cells, Zea promoted the nuclear translocation of NF-E2-related factor 2 (Nrf2) and induced mRNA and protein expression of phase II enzymes, the induction was suppressed by specific knockdown of Nrf2. Zea also effectively protected against *tert*-butyl hydroperoxide-induced mitochondrial dysfunction and apoptosis. Glutathione (GSH) as the most important antioxidant was also induced by Zea through Nrf2 activation in a time- and dose-dependent manner, whereas the protective effects of Zea were decimated by inhibition of GSH synthesis. Finally, Zea activated the PI3K/Akt and MAPK/ERK pathway, whereas only PI3K/Akt activation correlated with phase II enzymes induction and Zea protection. In further *in vivo* analyses, Zea showed effects of inducing phase II enzymes and increased GSH content, which contributed to the reduced lipid and protein peroxidation in the retina as well as the liver, heart, and serum of the Sprague–Dawley rats. For the first time, Zea is presented as a phase II enzymes inducer instead of being an antioxidant. By activating Nrf2-mediated phase II enzymes, Zea could enhance anti-oxidative capacity and prevent cell death both *in vivo* and *in vitro*.
Cell Death and Disease (2014) 5, e1218; doi:10.1038/cddis.2014.190; published online 8 May 2014
Subject Category: Cancer

Nuclear factor (erythroid-derived-2)-like 2, also known as Nrf2, is a member of the Cap 'n' Collar family of transcription factors that bind to antioxidant response elements and regulate the antioxidant response.[1,2] Nrf2 is tethered in the cytoplasm by the Keap1 protein under normal or unstressed conditions,[3] and Keap1 can target Nrf2 for ubiquitination by CUL3-ROC1 ligase and subsequent degradation by the proteasome.[4] Following activation, Nrf2 can translocate to the nucleus, where it binds to a small Maf protein and activates the transcription of target genes known as phase II enzymes, such as heme oxygenase-1 (HO-1),[5] NAD(P)H:quinone oxidoreductase (NQO-1),[6] and γ-glutamyl-cysteine ligase (GCL).[7] GCL is the rate-limiting enzyme regulating the synthesis of glutathione (GSH), which is one of the most important antioxidants *in vivo*,[8] and Nrf2 can influence GSH synthesis through regulating the expression of GCL catalytic (GCLc) modifier (GCLm) subunits. Reduced GSH in cells serves to maintain a reduced cellular environment and may also act as an important post-translational modification in a number of cellular proteins.[9] Therefore, an imbalance in GSH production has been implicated in the progression of various diseases, such as cancer,[10] obesity,[11] diabetes,[12] neurodegenerative disease,[13] and age-related macular degeneration (AMD).[14]

AMD is characterized by a progressive loss of central vision attributable to degenerative and neovascular changes at the ocular interface between the neural retina and the underlying choroid. AMD has been recognized as a threatening eye disease that affects millions of humans over the age of 65 years, especially in Europe and the United States.[15] Previous studies have indicated that the pathogenesis of AMD is strongly associated with chronic oxidative stress and inflammation, which ultimately lead to protein damage and aggregation and to degeneration of the retinal pigment epithelium (RPE).[16] As the major component of the anti-oxidant defense system, Nrf2 signaling in the RPE regulates GSH synthesis and protects against phtoto-oxidation.[17] In previous studies, we identified several Nrf2 activators, including alpha-tocopherol,[18] lipioc acid,[19] and hydroxytyrosol,[20] which all protect RPE cells from oxidative stress-induced cell death through Nrf2 activation, suggesting Nrf2 activation as a possible therapeutic target for treating oxidative diseases such as AMD.

[1]Key Laboratory of Biomedical Information Engineering of the Ministry of Education, School of Life Science and Technology, Xi'an Jiaotong University, Xi'an, China; [2]Center for Translational Medicine, Frontier Institute of Science and Technology, FIST, Xi'an Jiaotong University, Xi'an, China; [3]Center for Mitochondrial Biology and Medicine, Frontier Institute of Science and Technology, FIST, Xi'an Jiaotong University, Xi'an, China and [4]Jinan Central Hospital Affiliated to Shandong University, Jinan, China
*Corresponding author: Z Feng, Center for Mitochondrial Biology and Medicine, FIST, Xi'an Jiaotong University, 28 W, Xian-ning Road, Xi'an 710049, China.
Tel: +86 029 82665849; Fax: +86 029 82665849; E-mail: zhfeng@mail.xjtu.edu.cn
[5]These authors contributed equally to this work.

Zeaxanthin (Zea) is a well-known pigment that is commonly found in corn, carrots orange/yellow peppers, salmon, and egg yolks. The available evidence indicates a wide distribution of Zea in a number of body tissues, including the retina, where a high concentration is found.[21] The level of Zea in the retina declines significantly with increasing age in normal eyes,[22] and previous findings indicated that a lower concentration of Zea is associated with an increased risk of AMD.[23] However, daily supplements predominantly containing Zea are generally effective in increasing the macular pigment density and protecting against light-induced photoreceptor apoptosis.[24,25] Despite numerous *in vivo* and *in vitro* studies, our understanding of the mechanisms underlying the benefits of Zea in relation to AMD is still limited. Previous research has indicated that Zea functions as antioxidant to protect the lipid membrane and proteins through quenching singlet oxygen and scavenging reactive oxygen radicals.[26–28] In the present study, we aimed to investigate whether Zea can activate the Nrf2/keap1 pathway, which would, in turn, enhance the antioxidative capacity both *in vitro* and *in vivo*. We also investigated the potential mechanism underlying Zea activation of the Nrf2/keap1 pathway.

Results

Zea induces phase II enzyme expression. To investigate the effect of Zea on phase II enzymes, retinal pigmented epithelium cell line (ARPE-19) was used in current study. Cells were treated with Zea at 1, 10, 50 μM for 6 or 24 h. Real-time PCR analysis indicated a dose-dependent increase in the mRNA expression of HO-1, NQO-1, GCLc, and GCLm (Figures 1a–d). The protein levels of HO-1 and NQO-1 were further confirmed by western blot analysis (Figure 1e). In addition, a continuous time-dependent increase in NQO-1 protein contents was observed after treatment with 10 μM Zea for 6, 24, and 48 h, whereas the

highest level of HO-1 protein was found in the 6 h treatment (Figure 1f). These data suggested that Zea might activate phase II enzymes through increasing their expression at both the mRNA and protein levels.

Zea activates phase II enzymes through Nrf2 nuclear translocation. Nrf2 has been reported to be a key factor inducing phase II enzymes. To confirm that Zea activates these phase II enzymes through Nrf2, a specific Nrf2 siRNA was transfected into cells before Zea treatment. The siRNA caused significant inhibition of Nrf2 mRNA levels, which was not affected by the addition of Zea (Figure 2a). In addition, the induction of HO-1 and NQO-1 by Zea was efficiently abolished as a result of Nrf2 knockdown (Figures 2b and c). Similar results were obtained regarding protein contents (Figure 2d). Under normal conditions, Nrf2 is generally tethered in the cytoplasm by the Keap1 protein, and the activation of phase II enzymes can be achieved when Nrf2 is set free and translocates to the nucleus. We therefore sought to clarify the mechanism of Nrf2 activation by Zea. We found that neither dose-dependent (Figure 2e) nor time-dependent (Figure 2f) treatment with Zea had any effect on Nrf2 or Keap1 expression. However, the nuclear Nrf2 content was markedly increased in association with decreased cyto-Nrf2 levels after 6 h of Zea treatment (Figure 2g). Furthermore, an immunoprecipitation assay revealed that the 6 h Zea treatment greatly decreased the binding activity of Nrf2 to Keap1 (Figures 2h and i). Based on these observations, we inferred that Zea might disrupt the binding of Nrf2 with Keap1, freeing Nrf2 to undergo nuclear translocation.

Effects of Zea on tert-Butyl hydroperoxide (*t*-BHP)-induced oxidative stress and mitochondrial dysfunction. Although Zea has been tested in various models regarding its antioxidant activity, limited research has been performed in the
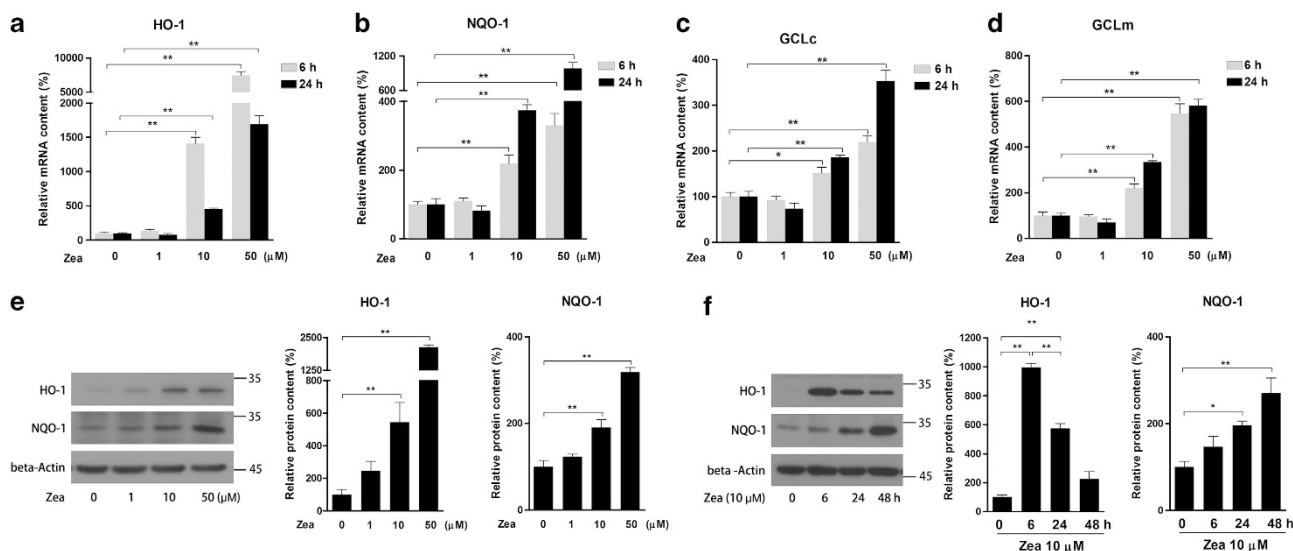

Figure 1 Effects of Zea on phase II enzyme expression. ARPE-19 cells were treated with Zea at the indicated concentrations (1, 10, 50 μM) for 6 or 24 h. The mRNA levels of the phase II enzymes HO-1 (**a**), NQO-1 (**b**), GCLc (**c**), and GCLm (**d**) were analyzed. The protein levels of HO-1 and NQO-1 were analyzed by western blotting, both after 24 h of treatment with Zea at different doses (**e**, left: western blot image, right: statistical analysis) and after treatment with 10 μM Zea for different time (**f**, left: western blot image, right: statistical analysis). All data are shown as mean $\pm$ S.E.M. The symbol '*' indicates statistical significance, as determined by one-way ANOVA (*$P < 0.05$, **$P < 0.01$, $n = 3$)
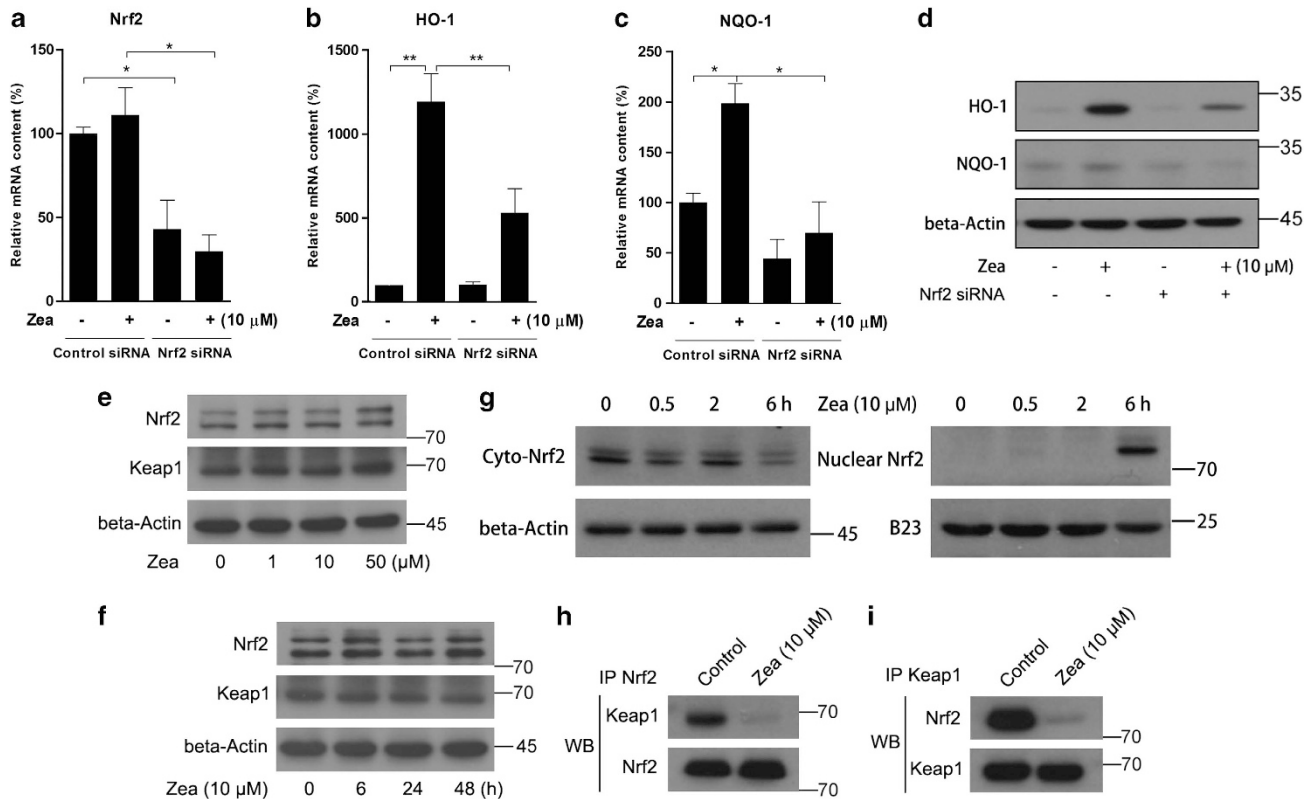
Figure 2 Zea activates phase II enzymes through Nrf2 nuclear translocation. ARPE-19 cells were transiently transfected with Nrf2 siRNA at 100 pmol per well in six-well plates for 24 h, followed by treatment with 10 μM Zea for 6 or 24 h. The mRNA levels of Nrf2 (a), HO-1 (b), and NQO-1 (c) were analyzed after 6 h of Zea treatment, and the protein levels of HO-1 and NQO-1 were analyzed after 24 h of Zea treatment (d). Protein levels of Nrf2 and Keap1 response to Zea dose-dependent and time-dependent effects were analyzed by western blot (e and f). Cyto- and nuclear Nrf2 levels after treatment with 10 μM Zea for 0.5, 2, or 6 h (g). Co-immunoprecipitation assays after 6 h of treatment with 10 μM Zea, antibodies against Nrf2 (h) and Keap1 (i) were used for immunoprecipitation, and the antibodies employed in the western blot analysis are indicated on the left side of the panel. All data are shown as mean ± S.E.M. The symbol '*' indicates statistical significance, as determined by one-way ANOVA (*$P < 0.05$, **$P < 0.01$, $n = 3$)

ARPE-19 cell t-BHP-induced oxidative stress model that we developed in the previous study.[29] Treatment with 300 μM t-BHP for 6 h was shown to induce significant oxidative damage. Pretreatment with Zea resulted in efficient protection against Cu-Zn SOD activity (Figure 3a), GPx activity (Figure 3b), and glutathione S-transferase (GST) activity (Figure 3c). Mitochondria are the predominant source of cellular energy and have a major part in t-BHP-induced cell toxicity. Our data showed that t-BHP challenge reduced the mitochondrial membrane potential (MMP), cell viability, and cellular ATP levels, which were all efficiently restored by pretreatment with Zea (Figures 3d–f). We therefore conclude that Zea conferred sufficient protection against t-BHP oxidative stress.

Effects of Zea on the t-BHP-induced activation of apoptosis. As a result of oxidative stress induced by t-BHP, ARPE-19 cells undergo apoptosis activation. Hence, we further investigated the effects of Zea on the activation of apoptosis. Hoechst staining revealed obvious apoptotic cells following t-BHP challenge, whereas Zea pretreatment resulted in efficient protection, inhibiting the activation of apoptosis (Figure 4a). It has been well documented that cleavage of poly (ADP-ribose) polymerase (PARP) and activation of caspases are important markers of apoptosis activation.[30,31] Here, PARP cleavage and caspase 9

activation were both observed under t-BHP challenge, and these changes were efficiently inhibited by Zea, indicating the sufficient inhibition of oxidative stress-induced cell apoptosis by Zea (Figures 4b and c).

GSH is the critical effector of the protective effect of Zea. As one of the most powerful antioxidants in living organisms, GSH was considered here because it is also a product of phase II enzymes. Zea treatment clearly increased the GSH content after 24 h (Figure 5a), with this increase beginning after 12 h of Zea exposure (Figure 5b). In contrast, Nrf2 knockdown apparently inhibited the induction of GSH by Zea treatment (Figure 5c). Zea pretreatment also resulted in significant protection of the t-BHP-induced GSH loss (Figure 5d), and this protection was abolished when cells were exposed to both Zea and BSO, a specific inhibitor of GSH synthesis (data not shown). Furthermore, the protective effects of Zea on cell viability and the MMP were abolished in the presence of BSO (Figures 5e and f). A similar result was obtained regarding the t-BHP-induced activation of cell apoptosis (Figure 5g). Thus, we concluded that GSH was the major effector in the protective effect of Zea.

Zea activates the Nrf2/Keap1 pathway through PI3/Akt activation. To investigate the pathways involved in the
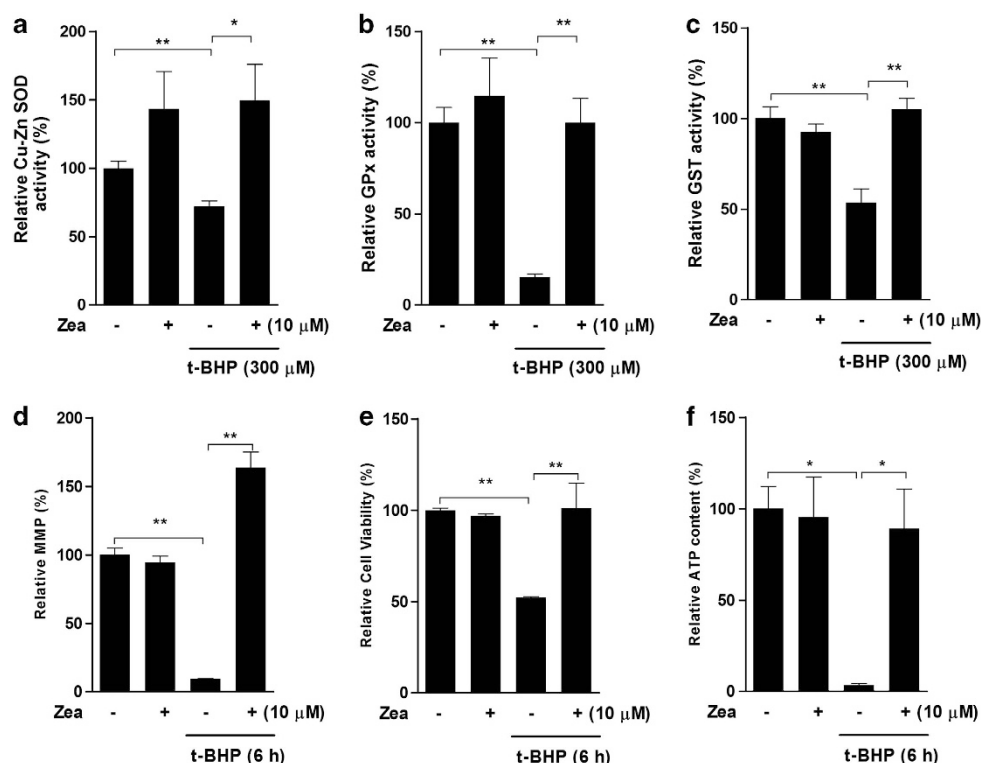
Figure 3 Zea confers protection against t-BHP-induced oxidative stress and mitochondrial dysfunction. ARPE-19 cells were treated with 10 μM Zea for 24 h, followed by 6 h of treatment with 300 μM t-BHP. Cu-Zn SOD activity (**a**), GPx activity (**b**), GST activity (**c**), the mitochondrial membrane potential (**d**), cell viability (**e**), and cellular ATP levels (**f**) were analyzed. All data are shown as mean ± S.E.M. The symbol '*' indicates statistical significance, as determined by one-way ANOVA (*$P<0.05$, **$P<0.01$, $n=3$)
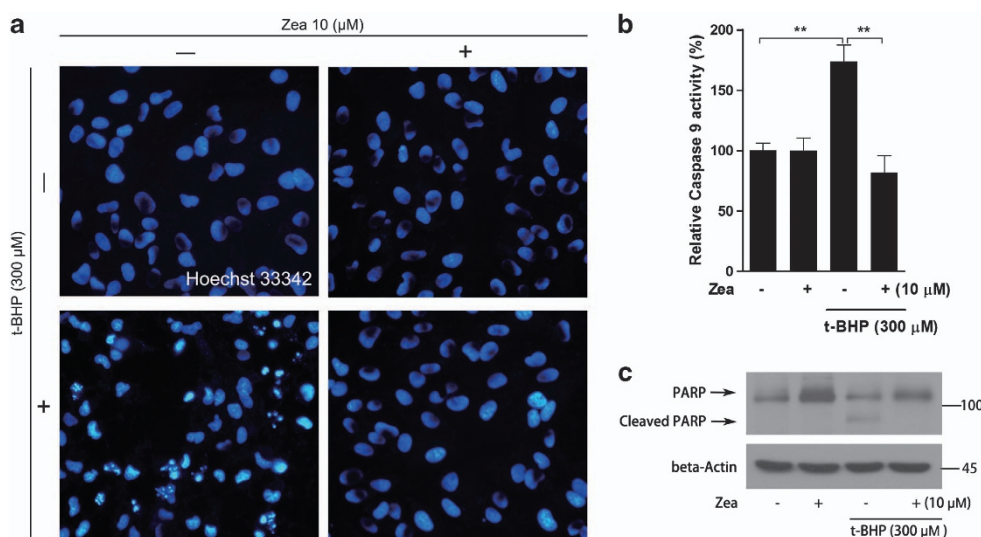

Figure 4 Zea inhibits the t-BHP-induced activation of apoptosis. ARPE-19 cells were treated with 10 μM Zea for 24 h, followed by 6 h of treatment with 300 μM t-BHP. Hoechst 33342 staining was performed to observe apoptotic cells (**a**). PARP cleavage was detected by western blotting (**c**), and caspase 9 activity was analyzed in live cells (**b**). All data are shown as mean ± S.E.M. The symbol '*' indicates statistical significance, as determined by one-way ANOVA (*$P<0.05$, **$P<0.01$, $n=3$)

activation of the Nrf2/Keap1 system, cells were treated with Zea for 5, 15, 30, or 120 min, and the phosphorylation of Akt, JNK, Erk1/2, and p38 was assessed via western blotting. As shown in Figure 6a, p-Akt and p-Erk1/2 showed obvious increases after 15 and 30 min of Zea treatment. Therefore, the specific inhibitors, such as LY294002 and U0126, were applied to cells treated with Zea. The induction of the Nrf2

targets HO-1 and NQO-1 by Zea was found to be significantly inhibited in the presence of LY294002, whereas no inhibitory effects were observed in the presence of U0126 (Figures 6b–d). Zea-induced GSH production was also decreased when Akt was inhibited using LY294002, whereas the inhibition of Erk1/2 using U0126 had no effect (Figure 6e). Furthermore, the protective effects of Zea on
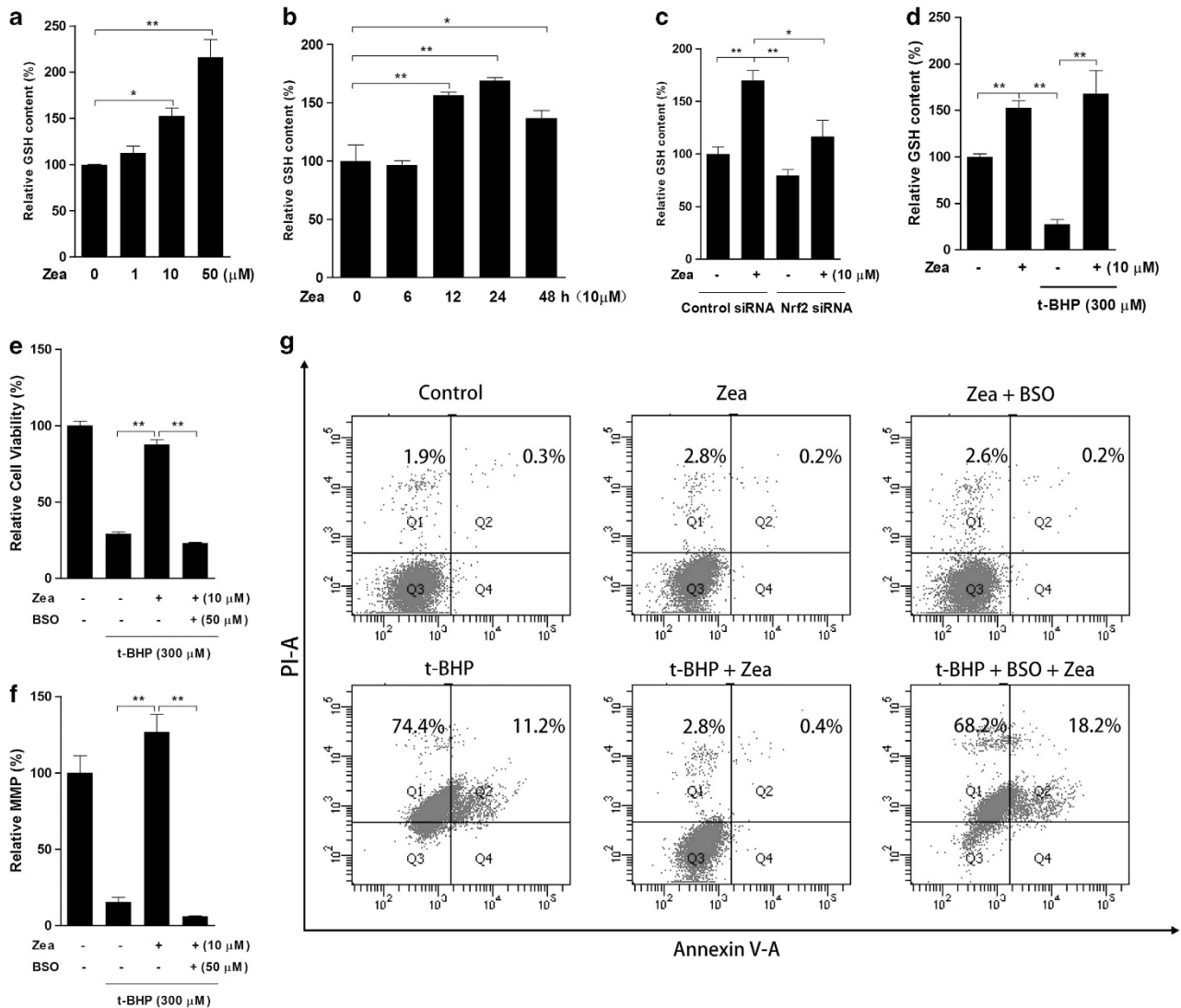
Figure 5 GSH is the critical effector of the protective effects of Zea. Total GSH levels were measured following the Zea treatment of ARPE-19 cells: (**a**) dose response—cells were treated with 1, 10, or 50 μM Zea for 24 h; (**b**) time response—cells were treated with 10 μM Zea for 6, 12, 24 or 48 h; (**c**) Nrf2 knockdown response—cells were transfected with Nrf2 siRNA for 24 h, followed by treatment with 10 μM Zea for an additional 24 h; (**d**) t-BHP response—cells were treated with 10 μM Zea for 24 h, followed by challenge with 300 μM t-BHP for an additional 6 h. In the presence of 50 μM BSO, cells were treated with 10 μM Zea for 24 h and then challenged with 300 μM t-BHP for an additional 6 h, after which cell viability (**e**), the mitochondrial membrane potential (**f**), and apoptosis activation (**g**) were analyzed. All data are shown as mean $\pm$ S.E.M. The symbol '*' indicates statistical significance, as determined by one-way ANOVA (*$P < 0.05$, **$P < 0.01$, $n = 3$)

cell viability and the MMP were abolished when Akt was inhibited, whereas Erk1/2 inhibition had no obvious effect (Figures 6f and g). We therefore concluded that the activation of the Nrf2/Keap1 system by Zea was dependent on the PI3K/Akt pathway, although Zea could potentially activate both Akt and Erk1/2.

Effects of Zea supplementation on the rat retina. Because Zea was found to activate phase II enzymes and to increase the antioxidative capacity in RPE cells, we further investigated the *in vivo* effects of Zea in the rat retina. As shown in Figure 7, the expression of Nrf2 target genes, such as HO-1 and NQO-1, was significantly increased by Zea supplementation in the rat retina (Figures 7a and b). The GSH content was also increased following Zea

supplementation (Figure 7c), whereas total Nrf2 expression was not affected. Similar to the *in vitro* results, Zea was found to significantly enhance Akt phosphorylation (Figures 7d and e), which might contribute to activation of the Nrf2/Keap1 pathway. Meanwhile, the contents of markers of lipid and protein peroxidation, 4-HNE (Figure 7f) and the carbonyl protein (Figures 7g and h), were significantly decreased by Zea treatment.

Effects of Zea supplementation on the rat liver and heart. To determine whether the retina was the only tissue affected by Zea, we tested rat liver and heart tissues and found increased levels of GSH (Figure 8a) and decreased levels of 4-HNE (Figure 8b) in the liver after Zea supplementation. Similar changes in the heart levels of GSH
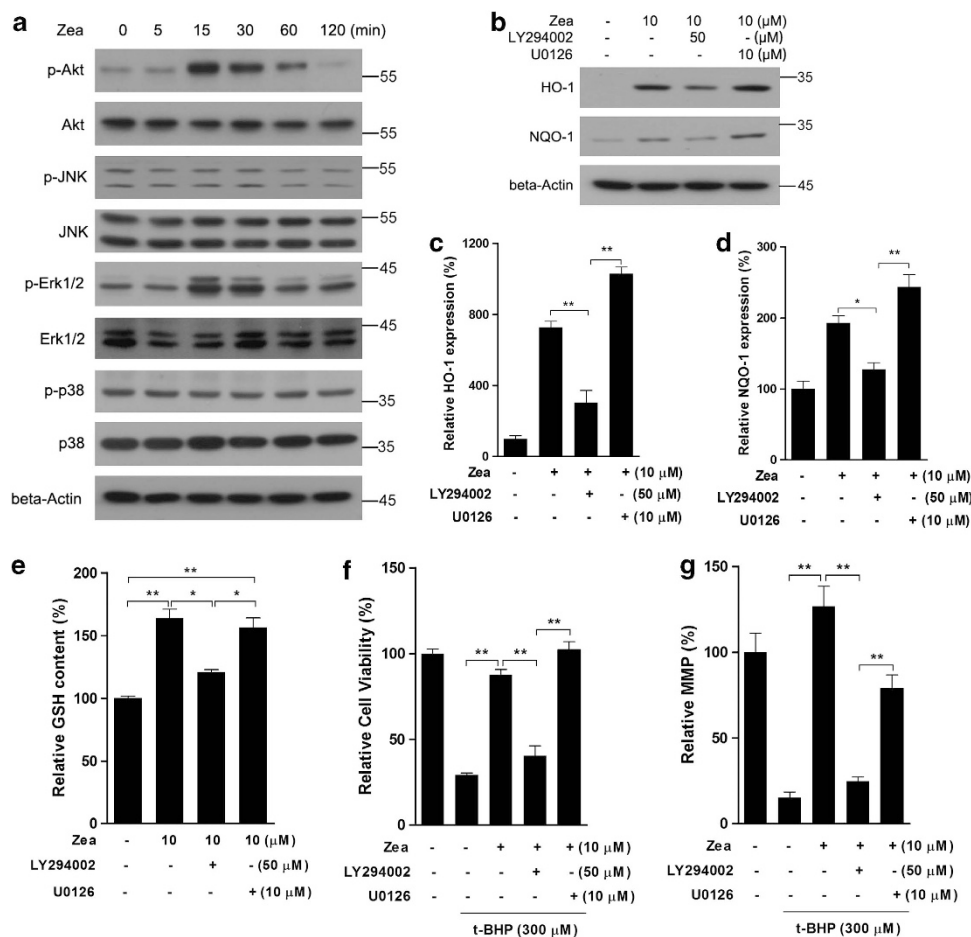
Figure 6 Zea activates the Nrf2/Keap1 pathway through PI3/Akt activation. ARPE-19 cells were treated with 10 μM Zea for the indicated time, and kinase activation was analyzed by western blotting (**a**). Cells were treated with 10 μM Zea in the presence of LY294002 or U0126 for 24 h, and the protein levels of HO-1 and NQO-1 were analyzed (**b**: western blot image; **c**: statistical analysis of HO-1 expression; **d**: statistical analysis of NQO-1 expression), GSH levels were also determined (**e**). Following co-treatment with Zea, LY294002, and U0126 for 24 h, cells were challenged with t-BHP for an additional 6 h, after which cell viability (**f**) and the mitochondrial membrane potential (**g**) were analyzed. All data are shown as mean $\pm$ S.E.M. The symbol '*' indicates statistical significance, as determined by one-way ANOVA (*$P < 0.05$, **$P < 0.01$, $n = 3$)

(Figure 8c) and 4-HNE (Figure 8d) were also observed. Moreover, the changes observed after Zea supplementation included increased GSH (Figure 8e), decreased 4-HEN (Figure 8f), and decreased carbonyl protein (Figures 8g and h) levels in rat serum, suggesting that Zea was able to efficiently reduce oxidative stress *in vivo*. Taken together, the GSH was suggested as the major effector of Zea for its protein against oxidative stress, and as shown in Figure 9, the induction of GSH increase was through activating PI3K/Akt pathway and promoting Nrf2 nuclear translocation.

Discussion

Zea and Lutein are well-known carotenoids that accumulate in the central retina, where they are collectively known as macular pigments. Increasing evidence indicates that these pigments are important for optimal visual performance because of their blue light-filtering properties.[32] It has also been suggested that supplementation of these pigments may provide benefits related to AMD because of their antioxidant capacity.[33,34] Although Zea and Lutein can be absorbed from daily supplementation, their concentrations in the retina

remain limited, and it remains a challenge to achieve good protection through direct reactions with oxidants alone. Therefore, we assumed that these pigments might activate another system, such as the phase II enzymes, to enhance the cellular antioxidative capacity, and we used Zea in the current study because it is more readily accessible in the market.

Following the treatment of ARPE-19 cells with Zea for various times and with various doses, we observed significant increases in phase II enzymes at both the mRNA and protein levels. We tested four phase II genes, GCLc, GCLm, HO-1, and NQO-1, in this study. GCLc and GCLm are the main enzymes that catalyze GSH synthesis, which has been indicated to decline with the progression of AMD.[14] HO-1, encoded by the *HMOX1* gene, can convert heme into the powerful pro-oxidant biliverdin, which is then transformed into bilirubin, a strong antioxidant,[35] and HO-1 levels have been found to decrease with age in RPE cells from eyes that show evidence of AMD.[36] Several nutrients with benefits related to AMD, such as curcumin and hydroxytyrosol, have been reported to induce HO-1 expression.[29,37] One report also showed that polymorphisms in NQO-1 are closely associated
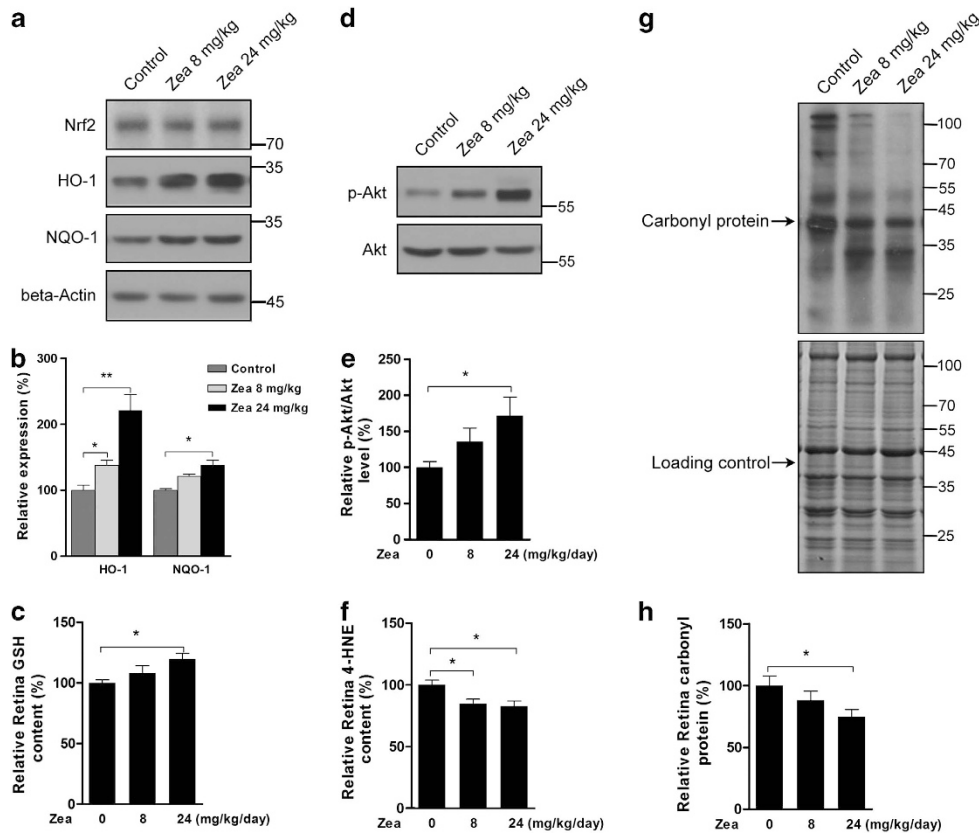
Figure 7 Zea activates phase II enzymes in the rat retina. SD rats were supplemented with Zea for 4 weeks, and their retinas were then isolated. Phase II enzyme protein expression (**a**: western blot image, **b**: statistical analysis), retina GSH contents (**c**), Akt activation (**d**: western blot image, **e**: statistical analysis), retina 4-HNE contents (**f**), and carbonyl protein levels (**g**: western blot image, **h**: statistical analysis) were analyzed. All data are shown as mean ± S.E.M. The symbol '*' indicates statistical significance, as determined by one-way ANOVA (*$P < 0.05$, **$P < 0.01$, $n = 8$)

with AMD risk.[38] Therefore, we assumed that the induction of phase II enzymes might be another mechanism accounting for the benefits of Zea against AMD. To further investigate this mechanism in detail, we first tested the Nrf2 protein, the key regulator of phase II enzyme activation. Nrf2 has been suggested to be released from Keap1, then translocate into the nucleus and bind to antioxidant response element to activate transcription. Therefore, we knocked down Nrf2 using a specific siRNA and found that the induction of HO-1 and NQO-1 by Zea was inhibited; this result confirmed previous conclusions regarding the regulation of phase II enzymes by Nrf2. In the present study, neither Nrf2 nor Keap1 protein levels were affected by Zea treatment. However, after 6 h, Zea treatment promoted Nrf2 nuclear translocation, accompanied by decreased cyto-Nrf2 contents. And the results of an immunoprecipitation assay indicated that the binding activity of Nrf2 to Keap1 was decreased. We therefore concluded that Zea could activate phase II enzyme activation through disruption of the binding of Nrf2 to Keap1.

It was previously reported that Zea supplementation could prevent photo-oxidative damage and modulate inflammatory responses in cultured ARPE-19 cells.[39] However, the effects of Zea on oxidative stress-induced mitochondrial dysfunction and the activation of apoptosis are poorly understood. As an important organelle in the cell, mitochondria are both the major source and a direct target of ROS. It has been

suggested that ROS-induced mitochondrial dysfunction has a critical role in blue light-induced retina cell apoptosis and AMD progression.[40,41] Therefore, treatment with 300 μM t-BHP for 6 h was used as a challenge to induce oxidative stress in ARPE-19 cells. As expected, the cellular anti-oxidative capacity, including the activities of Cu-Zn SOD, GPx, and GST, was decreased by t-BHP treatment, followed by impaired mitochondrial function, including decreases in the MMP, cell viability, and ATP contents. Zea treatment successfully restored these changes to normal levels. Furthermore, the cleavage of PARP was inhibited, and the activity of caspase 9 activity was normalized by Zea, and the activation of apoptosis was ultimately efficiently inhibited.

GSH is a well-known antioxidant that is synthesized by the phase II enzymes, GCLc and GCLm. Previous studies have indicated that MMP loss occurs downstream of GSH depletion, and GSH depletion may decrease MMP and increase the vulnerability of cells to apoptosis.[42,43] In the current study, we found that Zea could confer protection against both the MMP and GSH losses induced by t-BHP and further showed that Zea could induce GSH production through Nrf2 activation in a time- and dose-dependent manner. When GSH synthesis was inhibited by BSO, Zea failed to protect cell viability and the MMP. According to our flow cytometry analysis, t-BHP challenge triggered apoptosis in nearly 85% of cells. Treatment with Zea restored the level of cell apoptosis
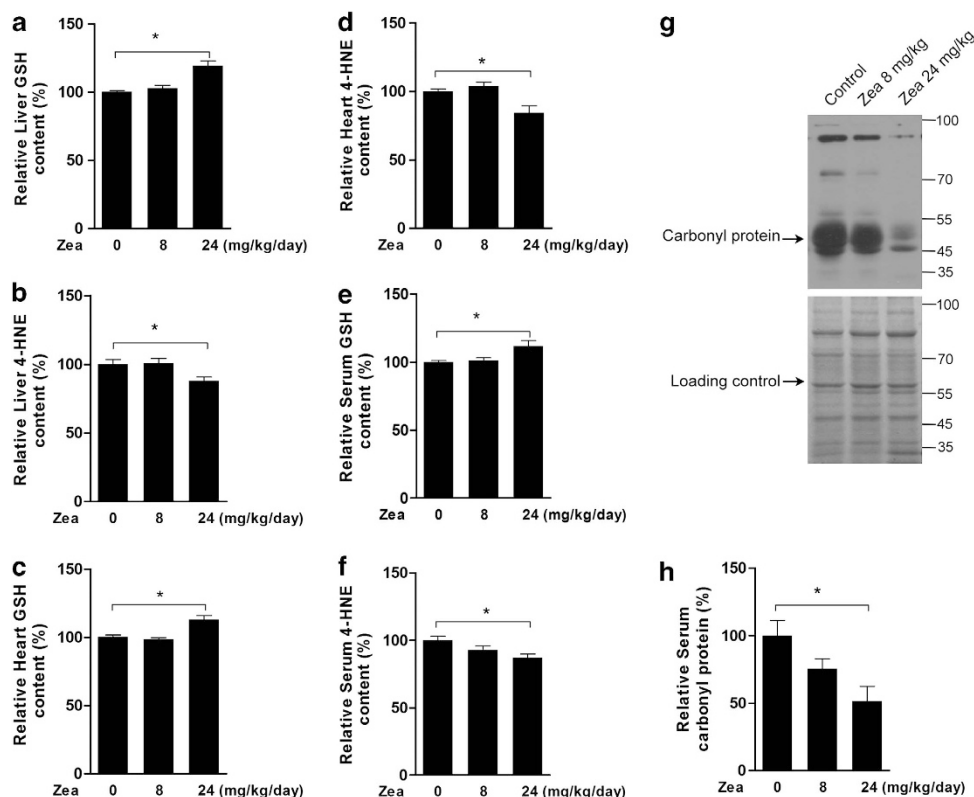
Figure 8 Effects of Zea in the rat liver, heart, and serum. SD rats were supplemented with Zea for 4 weeks, and their liver, heart, and serum were then collected. Liver GSH (**a**), liver 4-HNE (**b**), heart GSH (**c**), heart 4-HNE (**d**), serum GSH (**e**), serum 4-HNE (**f**), and serum carbonyl levels (**g**: Western blot image, **h**: statistical analysis) were analyzed. All data are shown as mean ± S.E.M. The symbol '*' indicates statistical significance, as determined by one-way ANOVA (*$P < 0.05$, **$P < 0.01$, $n = 8$)
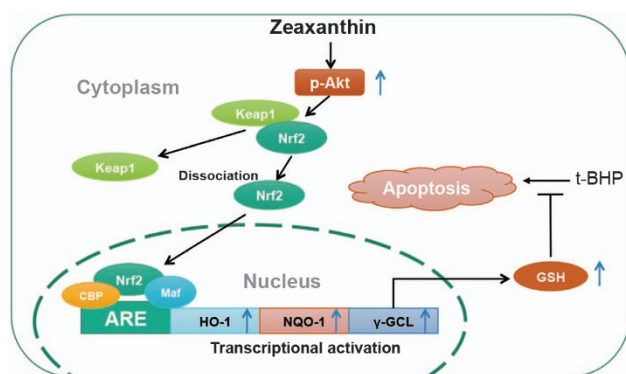

Figure 9 Possible mechanism of Zea protection against *t*-BHP-induced cell apoptosis. Zea could time and dose dependently induce expression of phase II enzymes through promoting Nrf2 nuclear translocation. GSH, the production of γ-GCL, was thereby increased, and accounted for anti-apoptotic effect of Zea. Meanwhile, the activation of PI3K/Akt pathway was found to work as upstream kinase regulating phase II enzymes expression and GSH production

to approximately 0.4%, which is quite similar to the level in normal cells. However, the percentage of apoptotic cells reached nearly 86% in the presence of BSO. We therefore concluded that Zea-induced GSH production was the major effector involved in the protection of mitochondrial function and inhibition of the activation of cell apoptosis.

The PI3K/Akt and MAPK pathways, including JNK, Erk, and p38 activation, have both been suggested as upstream

regulators of Nrf2.[44–46] In the current study, we observed activation of the PI3K/Akt and Erk pathways by Zea over time periods ranging from 5 to 120 min. To our surprise, the PI3K inhibitor LY294002 efficiently blocked the expression of HO-1 and NQO-1 induced by Zea, whereas the Erk inhibitor U0126 did not. Therefore, we inferred that the Nrf2 activation induced by Zea depends only on PI3K/Akt pathway. Accordingly, the Zea-induced increase in GSH was abolished by LY294002, but not U0126, and similar effects were found regarding the protective effects of Zea on cell viability and the MMP.

To further investigate the effects of Zea on phase II enzyme activation *in vivo,* SD rats were supplemented with Zea for 4 weeks. It was observed that Zea was able to induce Akt phosphorylation and increase antioxidant enzyme levels and GSH content in the retina, and lipid and protein peroxidation products including 4-HNE and carbonyl protein were therefore significantly reduced. It was interesting to find that the retina was not the only tissue affected by Zea, as an increased antioxidative capacity and decreased oxidative stress were also detected in the liver, heart, and serum of the rats. Between two tested Zea dosages, the higher dosage showed more significant effects. These data indicated that Zea can activate phase II enzymes *in vivo* and that the retina is not the only tissue that benefits from Zea treatment. However, whether the reduced oxidative stress was dependent on phase II enzymes induction requires further investigation, the application of Nrf2 knockout mice would be necessary, which is a limitation of the current study.

In conclusion, as shown in Figure 9, our results strongly suggest that Zea can activate the PI3K/Akt pathway and induce phase II enzyme expression through Nrf2 nuclear translocation, thereby protecting cells from oxidative stress-induced oxidative damage, mitochondrial dysfunction, and apoptosis. In addition, GSH, which is a critical antioxidant *in vivo,* was found to be the major effector involved in the protective effect of Zea. The *in vivo* effects of Zea regarding enhancement of the antioxidative capacity and reduction of oxidative stress were also confirmed. In addition to the retina, other tissues, including the liver and heart, were shown to benefit from Zea supplementation. Hence, we consider Zea to be an activator of the Nrf2/Keap1 pathway for the first time in the present work, which will potentially reveal further possible benefits of Zea related to the therapeutic treatment of diseases other than AMD.

Materials and Methods

Chemicals. Zea was purchased from Sigma (St. Louis, MO, USA); LY294002. U0126, an antibody against NQO-1, and anti-PARP were purchased from Cell Signaling Technology (Danvers, MA, USA). Anti-Keap1, anti-B23, anti-Akt, anti-p-Akt, anti-JNK, anti-p-JNK, anti-Erk1/2, anti-p-Erk1/2, anti-p38, anti-p-p38, anti-Nrf2, anti-heme oxygenase 1 (HO-1), and anti-β-actin were purchased from Santa Cruz Biotechnology (Santa Cruz, CA, USA). Other chemicals and reagents were purchased from Sigma if not otherwise indicated.

Cell culture. The human ARPE-19 cell line was obtained from ATCC and was cultured in DMEM-F12 supplemented with 10% fetal bovine serum, 0.348% sodium bicarbonate, 2 mM L-glutamine, 100 U/ml penicillin, and 100 μg/ml streptomycin. Cell cultures were maintained at 37 °C in a humidified atmosphere of 95% air and 5% CO_2. The medium was changed every 2 days. ARPE-19 cells were used within 10 passages.

MTT assay for cell viability. ARPE-19 cells were seeded in 96-well plates at a density of 4×10^4 cells per well for 24 h. After treatment with Zea, BSO, LY294002, and U0126, with or without t-BHP challenge, cell viability was determined by the addition of MTT (3-[4,5-dimethylthiazol-2-yl]-2,5-diphenylte-trazolium bromide), the Zea concentration zero contain the vehicle. Optical densities were read at 555 nm using a microplate spectrophotometer (Multiskan Ascent, Thermo Fisher Scientific Inc., Waltham, MA, USA).

JC-1 assay for the MMP. The MMP ($\Delta\Psi$) was assessed in live ARPE-19 cells using the lipophilic cationic probe 5,5′,6,6′-tetrachloro-1,1′,3,3′-tetraethyl-benzimidazolyl-carbocyanine iodide (JC-1). To perform quantitative fluorescence measurements, cells were rinsed once after JC-1 staining and scanned using a microplate fluorometer (Fluoroskan Ascent, Thermo Fisher Scientific Inc.) at a 488 nm excitation wavelength and 535 nm and 590 nm emission wavelengths to measure green and red JC-1 fluorescence, respectively. Each well was analyzed by measuring the intensity of 25 squares (1 mm^2 area each) arranged in a 5×5 rectangular array.

Enzyme activity assays. Cells were cultured in six-well plates. After treatment, the cells were ultrasonically lysed in 10 mM sodium phosphate buffer, pH 6.5. The total protein content of the cell lysates was quantified via the BCA method. GST activity was measured using 5 mg of protein, 1 mM GSH, 1 mM chloro-2,4-dinitrobenzene, and 3 mg/ml bovine serum albumin in 10 mM sodium phosphate buffer. The mixture was scanned at a wavelength of 340 nm for 5 min at 25 °C, as previously described.[18] The activities of Cu-Zn SOD and glutathione peroxidase (PGx) were analyzed using a commercial kit, following the manufacturer's protocol (Jiancheng Biochemical, Nanjing, China).

Measurement of intracellular ATP levels. Cells were cultured in six-well plates. After treatment, the cells were lysed using 0.5% Triton X-100 in 100 mM glycine buffer, pH 7.4. Assays to determine intracellular ATP levels were performed using an ATP bioluminescent assay kit (Sigma). ATP is consumed, and light is emitted when firefly luciferase catalyzes the oxidation of D-luciferin.[47]

Measurement of intracellular GSH levels. GSH levels were measured using 2,3-naphthalenedicarboxyaldehyde (NDA) as previously described.[48] A 20 μl sample plus 180 μl of NDA derivatization solution (50 mM Tris (pH 10), 0.5 N NaOH, and 10 mM NDA in Me_2SO; v/v/v, 1.4/0.2/0.2) was added to each well of a 96-well plate. The plate was covered to protect the wells from light and allowed to incubate at room temperature for 30 min. The NDA-GSH fluorescence intensity was measured (472 excitation/528 emission) using a microplate fluorometer (Fluoroskan Ascent, Thermo Fisher Scientific Inc.).

Flow cytometric analysis. Apoptosis was determined using the Annexin V-FITC apoptosis kit (Beyotime, Jiangsu, China), which detects cell surface changes that occur early in the apoptotic process. The assay was performed according to the manufacturer's instructions. Following growth and treatment, cells were collected and washed with PBS, and 1×10^5 cells were then incubated with 200 μl of the Annexin V-FITC solution for 10 min at room temperature, followed by 200 μl of a propidium iodide (PI) solution for another 10 min. The samples were subsequently analyzed using a FACScan flow cytometer (Becton Dickinson, Franklin Lakes, NJ, USA).

Caspase 9 activity assay. ARPE-19 cells were cultured in 96-well plates and allowed to reach 60–70% confluence. Then, the cells were treated with 10 μM Zea for 24 h, followed by t-BHP for an additional 6 h. Caspase 9 activity was analyzed with a commercial assay kit (Promega, Madison, WI, USA), following the manufacturer's protocol.

siRNA transfection. Transfection with an siRNA targeting Nrf2 was performed using a target sequence from human Nrf2, and control siRNA was used as a negative control. ARPE-19 cells were seeded at a density of 1.5×10^5 cells per well in six-well plates for transfection, western blot analysis, and real-time PCR assays. Transfection was performed using Lipofectamine 2000, as described in the supplier's manual. Briefly, appropriate amounts of Nrf2 siRNA and 5 μl of Lipofectamine 2000 in 250 μl of serum-free DMEM/F12 were prepared in separate RNase-free tubes. After a 5-min incubation, the siRNA and Lipofectamine were mixed, then incubated for an additional 20 min, and added to each well. A total of 100 pmol of siRNA was incubated per well for 24 h, and the cells were then treated with various compounds for the indicated analyses.

Real-time PCR. Total RNA was extracted from the cells using the TRIzol reagent (Invitrogen, Carlsbad, CA, USA), according to the manufacturer's protocol. Reverse transcription was performed using the PrimeScript RT-PCR Kit (TaKaRa, DaLian, China), followed by semiquantitative real-time PCR using specific primers. The primer sequences were as follows: Nrf2, 5′-TTCAGCAGCATCCTCTCCA CAG-3′ (forward) and 5′-GCATGCTGTTGCTGATACTGG-3′ (reverse); GCLc, 5′-GGCGATGAGGTGGAAATAC-3′ (forward) and 5′-AAAGGGTAGGATGGTTTGG-3′ (reverse); GCLm, 5′-ATCAAACTCTTCATCATCAAC-3′ (forward) and 5′-GATTAA CTCCATCTTCAATAGG-3′ (reverse); NQO-1, 5′-TGGCTAGGTATCATTCAACTC-3′ (forward) and 5′-CCTTAGGGCAGGTAGATTCAG-3′ (reverse); HO-1, 5′-GCCAG CAACAAAGTGCAAGAT-3′ (forward) and 5′-GGTAAGGAAGCCAGCCAAGAG-3′ (reverse); β-actin, 5-′CCACACCTTCTACAATGAGC-3′ (forward) and 5′-GGTCTC AAACATGATCTGGG-3′ (reverse).

Immunoprecipitation. Cells were grown to 80–90% confluence in 10 cm dishes and treated with Zea for 6 h. Total protein was collected using Western and IP lysis buffer (Beyotime). To avoid nonspecific binding, the lysates were precleared with protein G Sepharose (GE Healthcare, Piscataway, NJ, USA). The protein G Sepharose was subsequently removed via centrifugation at 4 °C for 10 min, and the supernatant was incubated with appropriate antibodies at 4 °C for 1 h and then with fresh protein G Sepharose at 4 °C overnight with gentle rotation. The samples were finally washed three times with IP lysis buffer, resuspended in SDS sample buffer, boiled, and centrifuged for 5 min. The supernatant was further analyzed by western blotting.

Western blot analyses. Samples were lysed with Western and IP lysis buffer (Beyotime). The lysates were then homogenized, and the homogenates were centrifuged at 13 000 × g for 15 min at 4 °C. Next, the supernatants were collected, and their protein concentrations were determined using the BCA Protein Assay kit (Pierce, Rockford, IL, USA, 23225). Equal amounts (20 μg) of each protein sample were applied to 10% SDS-PAGE gels, transferred to pure nitrocellulose membranes (Perkin-Elmer Life Sciences, Boston, MA, USA), and blocked with 5% non-fat milk. The membranes were incubated with anti-Keap1

(1 : 1000), anti-B23 (1 : 1000), anti-Akt (1 : 1000), anti-p-Akt (1 : 1000), anti-JNK (1 : 1000), anti-p-JNK (1 : 1000), anti-Erk1/2 (1 : 1000), anti-p-Erk1/2 (1 : 1000), anti-p38 (1 : 1000), anti-p-p38 (1 : 1000), anti-Nrf2 (1 : 1000), anti-HO-1 (1 : 1000), anti-histone H1 (1 : 1000), anti-NQO1 (1 : 1000), or anti-β-actin (1 : 10 000) at 4 °C overnight, followed by incubation with anti-rabbit or anti-mouse secondary antibodies at room temperature for 1 h. Chemiluminescent detection was performed using an ECL Western blotting detection kit (Pierce). Nuclear and cytoplasmic protein extracts were prepared with a Nuclear and Cytoplasmic Protein Extraction Kit (Beyotime Institute of Biotechnology), and Nrf2 was analyzed by western blotting. The results were analyzed using Quantity One software (Bio-Rad Life Science, Shanghai, China) to obtain the ratio of the optical density of the target protein to that of β-actin.

Animals and treatments. Four-week-old male SD rats were purchased from the SLAC Laboratory Animal Co. Ltd. (Shanghai, China). After 1 week of acclimatization, the rats were randomly divided into three groups ($n = 8$ in each group): rats fed a normal diet (control); rats fed a normal diet with daily oral gavage of a low dose of Zea (8 mg/kg/day); and rats fed a normal diet with daily oral gavage of a high dose of Zea (24 mg/kg/day). After 4 weeks of feeding, the rats were killed, and their serum and tissues including the retina, liver, and heart were isolated for analysis. All animals were housed in a temperature (22–28 °C)-controlled and humidity (60%)-controlled animal room and maintained under a 12 h light/12 h dark cycle (light from 0800 to 2000), with food and water provided during the experiments. All of the procedures were performed in accordance with the United States Public Health Services Guide for the Care and Use of Laboratory Animals, and all efforts were made to minimize the suffering and the number of animals used in this study.

Protein carbonylation assay. Protein carbonyls were assayed in soluble proteins using the Oxyblot protein oxidation detection kit (Cell Biolabs, San Diego, CA, USA). Protein carbonyls were labeled with 2,4-dinitrophenylhydrazine and detected by western blotting. As a negative loading control, equal amounts of the samples were subjected to 10% SDS-PAGE and stained with Coomassie brilliant blue.

Statistical analysis. Data are presented as the means ± S.E.M. Statistical significance was evaluated using a one-way ANOVA followed by LSD *post-hoc* analysis. For all comparisons, the level of significance was set at $P < 0.05$.

Conflict of Interest

The authors declare no conflict of interest.

1. Li W, Kong AN. Molecular mechanisms of Nrf2-mediated antioxidant response. *Mol Carcinog* 2009; **48**: 91–104.
2. Nguyen T, Nioi P, Pickett CB. The Nrf2-antioxidant response element signaling pathway and its activation by oxidative stress. *J Biol Chem* 2009; **284**: 13291–13295.
3. Itoh K, Wakabayashi N, Katoh Y, Ishii T, Igarashi K, Engel JD et al. Keap1 represses nuclear activation of antioxidant responsive elements by Nrf2 through binding to the amino-terminal Neh2 domain. *Genes Dev* 1999; **13**: 76–86.
4. Furukawa M, Xiong Y. BTB protein Keap1 targets antioxidant transcription factor Nrf2 for ubiquitination by the Cullin 3-Roc1 ligase. *Mol Cell Biol* 2005; **25**: 162–171.
5. Alam J, Stewart D, Touchard C, Boinapally S, Choi AM, Cook JL. Nrf2, a Cap'n'Collar transcription factor, regulates induction of the heme oxygenase-1 gene. *J Biol Chem* 1999; **274**: 26071–26078.
6. Venugopal R, Jaiswal AK. Nrf1 and Nrf2 positively and c-Fos and Fra1 negatively regulate the human antioxidant response element-mediated expression of NAD(P)H:quinone oxidoreductase1 gene. *Proc Natl Acad Sci USA* 1996; **93**: 14960–14965.
7. Suh JH, Shenvi SV, Dixon BM, Liu H, Jaiswal AK, Liu RM et al. Decline in transcriptional activity of Nrf2 causes age-related loss of glutathione synthesis, which is reversible with lipoic acid. *Proc Natl Acad Sci USA* 2004; **101**: 3381–3386.
8. Botta D, White CC, Vliet-Gregg P, Mohar I, Shi S, McGrath MB et al. Modulating GSH synthesis using glutamate cysteine ligase transgenic and gene-targeted mice. *Drug Metab Rev* 2008; **40**: 465–477.
9. Townsend DM, Tew KD, Tapiero H. The importance of glutathione in human disease. *Biomed Pharmacother* 2003; **57**: 145–155.
10. Smaaland R, Abrahamsen JF, Svardal AM, Lote K, Ueland PM. DNA cell cycle distribution and glutathione (GSH) content according to circadian stage in bone marrow of cancer patients. *Br J Cancer* 1992; **66**: 39–45.
11. Sastre J, Pallardo FV, Llopis J, Furukawa T, Vina JR, Vina J. Glutathione depletion by hyperphagia-induced obesity. *Life Sci* 1989; **45**: 183–187.
12. Beard KM, Shangari N, Wu B, O'Brien PJ. Metabolism, not autoxidation, plays a role in alpha-oxoaldehyde- and reducing sugar-induced erythrocyte GSH depletion: relevance for diabetes mellitus. *Mol Cell Biochem* 2003; **252**: 331–338.
13. Zeevalk GD, Manzino L, Sonsalla PK, Bernard LP. Characterization of intracellular elevation of glutathione (GSH) with glutathione monoethyl ester and GSH in brain and neuronal cultures: relevance to Parkinson's disease. *Exp Neurol* 2007; **203**: 512–520.
14. Samiec PS, Drews-Botsch C, Flagg EW, Kurtz JC, Sternberg Jr P, Reed RL et al. Glutathione in human plasma: decline in association with aging, age-related macular degeneration, and diabetes. *Free Radic Biol Med* 1998; **24**: 699–704.
15. Kokotas H, Grigoriadou M, Petersen MB. Age-related macular degeneration: genetic and clinical findings. *Clin Chem Lab Med* 2011; **49**: 601–616.
16. Kinnunen K, Petrovski G, Moe MC, Berta A, Kaarniranta K. Molecular mechanisms of retinal pigment epithelium damage and development of age-related macular degeneration. *Acta Ophthalmol* 2012; **90**: 299–309.
17. Gao X, Talalay P. Induction of phase 2 genes by sulforaphane protects retinal pigment epithelial cells against photooxidative damage. *Proc Natl Acad Sci USA* 2004; **101**: 10446–10451.
18. Feng Z, Liu Z, Li X, Jia H, Sun L, Tian C et al. alpha-Tocopherol is an effective Phase II enzyme inducer: protective effects on acrolein-induced oxidative stress and mitochondrial dysfunction in human retinal pigment epithelial cells. *J Nutr Biochem* 2010; **21**: 1222–1231.
19. Jia L, Liu Z, Sun L, Miller SS, Ames BN, Cotman CW et al. Acrolein, a toxicant in cigarette smoke, causes oxidative damage and mitochondrial dysfunction in RPE cells: protection by (R)-alpha-lipoic acid. *Invest Ophthalmol Vis Sci* 2007; **48**: 339–348.
20. Zou X, Feng Z, Li Y, Wang Y, Wertz K, Weber P et al. Stimulation of GSH synthesis to prevent oxidative stress-induced apoptosis by hydroxytyrosol in human retinal pigment epithelial cells: activation of Nrf2 and JNK-p62/SQSTM1 pathways. *J Nutr Biochem* 2012; **23**: 994–1006.
21. Ma L, Lin XM. Effects of lutein and zeaxanthin on aspects of eye health. *J Sci Food Agric* 2010; **90**: 2–12.
22. Gellermann W, Ermakov IV, Ermakova MR, McClane RW, Zhao DY, Bernstein PS. In vivo resonant Raman measurement of macular carotenoid pigments in the young and the aging human retina. *J Opt Soc Am A Opt Image Sci Vis* 2002; **19**: 1172–1186.
23. Bone RA, Landrum JT, Dixon Z, Chen Y, Llerena CM. Lutein and zeaxanthin in the eyes, serum and diet of human subjects. *Exp Eye Res* 2000; **71**: 239–245.
24. Bone RA, Landrum JT, Cao Y, Howard AN, Alvarez-Calderon F. Macular pigment response to a supplement containing meso-zeaxanthin, lutein and zeaxanthin. *Nutr Metab* 2007; **4**: 12.
25. Thomson LR, Toyoda Y, Langner A, Delori FC, Garnett KM, Craft N et al. Elevated retinal zeaxanthin and prevention of light-induced photoreceptor cell death in quail. *Invest Ophthalmol Vis Sci* 2002; **43**: 3538–3549.
26. Wrona M, Rozanowska M, Sarna T. Zeaxanthin in combination with ascorbic acid or alpha-tocopherol protects ARPE-19 cells against photosensitized peroxidation of lipids. *Free Radic Biol Med* 2004; **36**: 1094–1101.
27. Baroli I, Do AD, Yamane T, Niyogi KK. Zeaxanthin accumulation in the absence of a functional xanthophyll cycle protects Chlamydomonas reinhardtii from photooxidative stress. *Plant Cell* 2003; **15**: 992–1008.
28. Nakajima Y, Shimazawa M, Otsubo K, Ishibashi T, Hara H. Zeaxanthin, a retinal carotenoid, protects retinal cells against oxidative stress. *Curr Eye Res* 2009; **34**: 311–318.
29. Zou X, Feng Z, Li Y, Wang Y, Wertz K, Weber P et al. Stimulation of GSH synthesis to prevent oxidative stress-induced apoptosis by hydroxytyrosol in human retinal pigment epithelial cells: activation of Nrf2 and JNK-p62/SQSTM1 pathways. *J Nutr Biochem* 2012; **23**: 994–1006.
30. Boulares AH, Yakovlev AG, Ivanova V, Stoica BA, Wang G, Iyer S et al. Role of poly(ADP-ribose) polymerase (PARP) cleavage in apoptosis. Caspase 3-resistant PARP mutant increases rates of apoptosis in transfected cells. *J Biol Chem* 1999; **274**: 22932–22940.
31. Wu GS, Ding Z. Caspase 9 is required for p53-dependent apoptosis and chemosensitivity in a human ovarian cancer cell line. *Oncogene* 2002; **21**: 1–8.
32. Junghans A, Sies H, Stahl W. Macular pigments lutein and zeaxanthin as blue light filters studied in liposomes. *Arch Biochem Biophys* 2001; **391**: 160–164.
33. Chucair AJ, Rotstein NP, Sangiovanni JP, During A, Chew EY, Politi LE. Lutein and zeaxanthin protect photoreceptors from apoptosis induced by oxidative stress: relation with docosahexaenoic acid. *Invest Ophthalmol Vis Sci* 2007; **48**: 5168–5177.
34. Fernandez-Robredo P, Recalde S, Arnaiz G, Salinas-Alaman A, Sadaba LM, Moreno-Orduna M et al. Effect of zeaxanthin and antioxidant supplementation on vascular endothelial growth factor (VEGF) expression in apolipoprotein-E deficient mice. *Curr Eye Res* 2009; **34**: 543–552.
35. Mishra M, Ndisang JF. A critical and comprehensive insight on heme oxygenase and related products including carbon monoxide, bilirubin, biliverdin and ferritin in type-1 and type-2 diabetes. *Curr Pharm Design* 2014; **20**: 1370–1391.

36. Frank RN, Amin RH, Puklin JE. Antioxidant enzymes in the macular retinal pigment epithelium of eyes with neovascular age-related macular degeneration. *Am J Ophthalmol* 1999; **127**: 694–709.

37. Mandal MN, Patlolla JM, Zheng L, Agbaga MP, Tran JT, Wicker L *et al.* Curcumin protects retinal cells from light-and oxidant stress-induced cell death. *Free Radic Biol Med* 2009; **46**: 672–679.

38. Synowiec E, Sliwinski T, Danisz K, Blasiak J, Sklodowska A, Romaniuk D *et al.* Association between polymorphism of the NQO1, NOS3 and NFE2L2 genes and AMD. *Front Biosci* 2013; **18**: 80–90.

39. Bian Q, Gao S, Zhou J, Qin J, Taylor A, Johnson EJ *et al.* Lutein and zeaxanthin supplementation reduces photooxidative damage and modulates the expression of inflammation-related genes in retinal pigment epithelial cells. *Free Radic Biol Med* 2012; **53**: 1298–1307.

40. King A, Gottlieb E, Brooks DG, Murphy MP, Dunaief JL. Mitochondria-derived reactive oxygen species mediate blue light-induced death of retinal pigment epithelial cells. *Photochem Photobiol* 2004; **79**: 470–475.

41. Schrier SA, Falk MJ. Mitochondrial disorders and the eye. *Curr Opin Ophthalmol* 2011; **22**: 325–331.

42. Swamy SM, Huat BT. Intracellular glutathione depletion and reactive oxygen species generation are important in alpha-hederin-induced apoptosis of P388 cells. *Mol Cell Biochem* 2003; **245**: 127–139.

43. Bojes HK, Feng X, Kehrer JP, Cohen GM. Apoptosis in hematopoietic cells (FL5.12) caused by interleukin-3 withdrawal: relationship to caspase activity and the loss of glutathione. *Cell Death Differ* 1999; **6**: 61–70.

44. Nakaso K, Yano H, Fukuhara Y, Takeshima T, Wada-Isoe K, Nakashima K. PI3K is a key molecule in the Nrf2-mediated regulation of antioxidative proteins by hemin in human neuroblastoma cells. *FEBS Lett* 2003; **546**: 181–184.

45. Filomeni G, Piccirillo S, Rotilio G, Ciriolo MR. p38(MAPK) and ERK1/2 dictate cell death/survival response to different pro-oxidant stimuli via p53 and Nrf2 in neuroblastoma cells SH-SY5Y. *Biochem Pharmacol* 2012; **83**: 1349–1357.

46. Vari R, D'Archivio M, Filesi C, Carotenuto S, Scazzocchio B, Santangelo C *et al.* Protocatechuic acid induces antioxidant/detoxifying enzyme expression through JNK-mediated Nrf2 activation in murine macrophages. *J Nutr Biochem* 2011; **22**: 409–417.

47. Li X, Liu Z, Luo C, Jia H, Sun L, Hou B *et al.* Lipoamide protects retinal pigment epithelial cells from oxidative stress and mitochondrial dysfunction. *Free Radic Biol Med* 2008; **44**: 1465–1474.

48. White CC, Viernes H, Krejsa CM, Botta D, Kavanagh TJ. Fluorescence-based microtiter plate assay for glutamate-cysteine ligase activity. *Anal Biochem* 2003; **318**: 175–180.